Steam Gasification of a Cellulose Surrogate over a Fluidizable Ni/α-Alumina Catalyst: A Kinetic Model

Enrique Salaices and Hugo de Lasa
Chemical Reactor Engineering Centre, The University of Western Ontario, London, Ontario, Canada N6A5B8

Benito Serrano
Programa Ingenieria Quimica, Universidad Autonoma de Zacatecas, Zacatecas, Mexico

DOI 10.1002/aic.12696
Published online July 13, 2011 in Wiley Online Library (wileyonlinelibrary.com).

Catalytic steam gasification of a cellulose surrogate using a fluidizable Ni/α-alumina catalyst is presented. Experiments were carried out in the CREC fluidized riser simulator. On this basis, a reaction network and a kinetic model for biomass catalytic steam gasification were proposed. This kinetic model was developed using a sound reaction engineering approach where reaction rates for various species are the result of the algebraic addition of dominant reactions. The modeling procedure also included the decoupled determination of intrinsic kinetic parameters and adsorption constants as allowed in the CREC riser simulator. The implemented approach eliminates overparametrization with successfully parameter correlation. Numerical regression of the experimental data led to intrinsic kinetic parameters with narrow spans showing that the proposed kinetic model satisfactorily describe the catalytic conversion of glucose under the selected gasification conditions. © 2011 American Institute of Chemical Engineers *AIChE J,* 58: 1588–1599, 2012

Keywords: kinetics, biomass, steam gasification, Ni/α-Al_2O_3 catalyst

Introduction

Biomass steam gasification has become an area of growing interest because it produces a gaseous fuel with relatively higher hydrogen content that could be used for industrial applications, both for highly efficient electricity production and as a feedstock for chemical synthesis. Furthermore, steam gasification has other advantages in that (1) it produces a gas with higher heating value, (2) it reduces the diluting effect of N_2 from air, and (3) it eliminates the need for an expensive oxygen plant when both air and oxygen are used as gasification mediums.[1] Catalytic steam gasification of biomass in fluidized beds is a promising approach given its rapid biomass heating, its effective heat and mass transfer between reacting phases, and its uniform reaction temperature.[2] Moreover, fluidized beds tolerate wide variations in fuel quality as well as broad particle-size distributions.

The steam gasification of biomass is a complex network of heterogeneous reactions. Primary reactions break down the vaporized biomass molecules, forming coke and permanent gases

$$C_x H_y O_z + \omega H_2O \xrightarrow{\text{heat}} \alpha H_2 + \beta CO + \gamma CO_2 + \psi H_2O + \varsigma C_n H_{2m} + \Omega C(s) \quad (1)$$

Secondary reactions crack the higher hydrocarbons into gases that further combust or become reduced

$$C_n H_{2m} + nH_2O \longrightarrow nCO + (n+m) H_2 \quad (2)$$

Correspondence concerning this article should be addressed to H. de Lasa at hdelas@eng.uwo.ca.

Furthermore, permanent gases react to alter the gas composition depending on gasifier conditions

$$CO + H_2O \longleftrightarrow H_2 + CO_2 \quad (3)$$

$$CH_4 + H_2O \longleftrightarrow CO + 3H_2 \quad (4)$$

$$CH_4 + CO_2 \longleftrightarrow 2CO + 2H_2 \quad (5)$$

$$C + H_2O \longleftrightarrow H_2 + CO \quad (6)$$

$$C + CO_2 \longleftrightarrow 2CO \quad (7)$$

$$C + 2H_2 \longleftrightarrow CH_4 \quad (8)$$

Experimental data in a previous study demonstrates the shortcomings of equilibrium models for gasifiers with reaction times shorter than 10 s, and the need for nonequilibrium models to describe gasifier performance at such conditions.[3]

Various kinetic models of different complexity describing the gasification of various biomass feeds were proposed in the literature.[4–9] These models utilize subsets of reactions under a wide range of gasification conditions. These authors concluded that the following reactions have to be considered; (1) the kinetically limited steam reforming of methane, and (2) the close to equilibrium water-gas shift reaction.[10–12,14–16]

One of the main shortcomings of the proposed gasification kinetic models is given by the fact that they lump together a complex network of heterogeneous reactions in one single kinetic rate equation. While this in principle circumvents the overparameterization problem, the resulting rate equation provides an empirically fitted kinetic model. This model has little or no connection with the phenomenological events of either adsorption or reaction taking place.

Thus, one of the goals set for this study is to overcome this dilemma demonstrating the viability of establishing, as it is shown in the upcoming sections, that kinetic models for biomass catalytic steam gasification can be developed using a coherent reaction engineering approach where reaction rates for various species are the result of the algebraic addition (*additive effect*) of the dominant reactions as follows:

$$r_{j,i} = \sum_{i}^{n} \frac{v_{j,i}}{v_{j,r}} r_{j,r} \quad (9)$$

where $v_{j,i}$, and $r_{j,i}$ are the stoichiometric coefficients and reaction rates for species i in reaction j and $v_{j,r}$, and $r_{j,r}$ are the stoichiometric coefficients and reaction rates for the reference species r in reaction j.

In the case of catalytic reactions, each one of these rates can be frequently modeled using a Langmuir-Hinshelwood type rate equation, which takes into consideration the adsorption of the reactants on the catalyst surface as well as the reaction kinetics. The general form of a Langmuir-Hinshelwood for this system is given by Ollis et al.[19]

$$r_i = \frac{k_i^k K_i^A p_i}{\left(1 + \sum_{j=1}^{n} K_j^A p_j\right)^{m'}} \quad (10)$$

where r_i is the rate of reaction of component i in mol/g_{cat} min, K_i^k is the kinetic constant for component i in mol/g_{cat} min, K_i^A is the adsorption constant for component i in 1/atm, p is the partial pressure of component i in atm. The term n is the number of chemical species, while j is a subscript to denote each component in the denominator term, and m' the number of catalyst sites involved in the catalytic reaction.

Thus, if one uses a Langmuir-Hinselwood model for each one of the dominant WGS,[32] SMR[33–36] and DMR[37] reactions, and do this in agreement with literature reported kinetics the following can be considered[31]

$$r_{WGS,H_2} = \frac{k_{WGS} K_{H_2O}^A K_{CO}^A p_{CO}\, p_{H_2O}}{\left(1 + K_{CH_4}^A p_{CH_4} + K_{CO_2}^A p_{CO_2}\right)^2} \left(1 - \frac{p_{H_2}\, p_{CO2}}{K_{WGS}\, p_{CO}\, p_{H_2O}}\right) \quad (11)$$

$$r_{SR,CO} = \frac{k_{SR} K_{CH_4}^A K_{H_2O}^A p_{CH_4}\, p_{H_2O}}{\left(1 + K_{CH_4}^A p_{CH_4} + K_{CO_2}^A p_{CO_2}\right)^4} \left(1 - \frac{p_{CO}\, p_{H_2}^3}{K_{SR}\, p_{CH_4}\, p_{H_2O}}\right) \quad (12)$$

$$r_{DRM,CH_4} = -\frac{k_{DRM} K_{CO_2}^A K_{CH_4}^A p_{CO_2}\, p_{CH_4}}{\left(1 + K_{CH_4}^A p_{CH_4} + K_{CO_2}^A p_{CO_2}\right)^4} \times \left(1 - \frac{p_{CO}^2\, p_{H_2}^2}{K_{DRM}\, p_{CO_2}\, p_{CH_4}}\right) \quad (13)$$

It can be noticed that each of these equations include relevant physicochemical intrinsic kinetic parameters k_j, and adsorption constants K_j^A.

Materials, Experimental Setup and Methodology

Catalyst preparation

The α-alumina supported nickel catalyst was prepared according to the incipient wetness technique. The α-alumina, which acts as support to the active metal, was obtained from Stream Chemicals, Inc., with 65% Al_2O_3, 34.8% H_2O, and 0.15% Na_2O composition. The α-alumina was calcined *priori* to metal loading impregnation. Calcination consisted of heating the α-alumina in a furnace oven to a temperature of 1000°C for 8 h. This process removed excess water and eliminated potential thermal instability in the alumina powder. Nickel loading was achieved according to the following steps; (a) the alumina powder was placed into a quartz flask, (b) a magnetic stirrer was inserted into the flask and then the flask was sealed with a rubber septum, and (c) the system was kept under 250 mm Hg vacuum. A nickel-nitrate solution was prepared by dissolving nickel-nitrate hexahydrate, (Ni $(NO_3)_3{\cdot}6H_2O$), powder in water. 0.8 mL of water was used for every gram of α-alumina support. The amount of desired nickel-nitrate hexahydrate powder to be dissolved in water and to be added to the support was calculated by the formula $m_{Ni(NO_3)3{\cdot}6H_2O} = \frac{x_{Ni}\, MW_{Ni(NO_3)3{\cdot}6H_2O}\, m_{Al_2O_3}}{MW_{Ni}\, x_{purity}}$ where $m_{Ni(NO3)3{\cdot}6H_2O}$ represents the mass of nickel-nitrate hexahydrate added x_{Ni}, the percent metal loading $MW_{Ni(NO_3)3{\cdot}6H_2O}$, the molecular weight of nickel-nitrate hexahydrate $m_{A1_2O_3}$, the mass of α-alumina support MW_{Ni} the molecular weight of nickel, and x_{purity} the percentage purity of nickel-nitrate hexahydrate. The nickel solution was introduced into a flask using a syringe. A magnetic stirrer was used to mix the

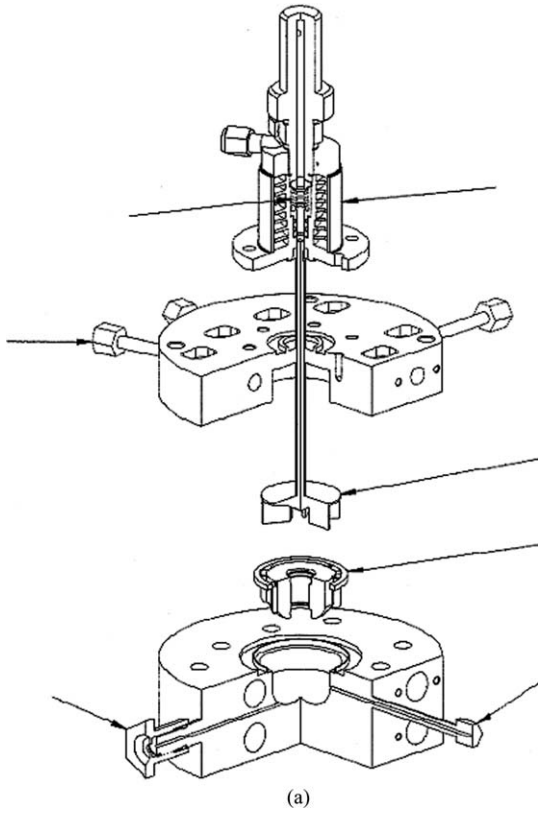

Figure 1. (a) Schematic diagram of the CREC riser simulator: quarter section view, upper and lower shells exposed, and (b) CREC riser simulator and sampling system as currently implemented in CREC-UWO (Salaices[31]).

[Color figure can be viewed in the online issue, which is available at wileyonlinelibrary.com.]

impregnated α-alumina until the mixture was homogeneous in color (uniformly colored emerald green paste). In order to dry the impregnated α-alumina solution, the resulting paste was heated in a furnace oven to a temperature of 140°C at a 20°C/h heating rate during 6 h. Following this and in order to decompose the nickel nitrate on α-alumina support, the catalyst powder was placed in the specially designed fluidized-bed reactor placed in a furnace oven. The temperature was kept at 750°C for a period of 8 h. During this time, a stream of gas containing hydrogen flowed through the bed of catalyst. The nickel nitrate decomposed first to nickel oxide with the nickel oxide being reduced in a second step. Water and HNO_3 vapors exited the fluidized-bed reactor through an exhaust stream. The HNO_3 in the exhaust stream was then scrubbed in a sodium hydroxide solution inside the fume hood. The HNO_3 reacted with the sodium hydroxide forming sodium nitrate and water. Multiple metal loadings were accomplished according to the aforementioned procedure. Each metal loading presumably added 2.5 wt % nickel to α-alumina support. When the desired metal loading was reached, the impregnated α-alumina solution was calcined under an air atmosphere. The catalyst was placed in the furnace oven and heated to a temperature of 750°C for 8 h. Additional information regarding the incipient wetness technique is provided in Salaices[31].

Catalyst characterization

Physical and chemical analyses were conducted to predict the catalytic performance of Ni/α-alumina including: Particle-size distribution (PSD), apparent density (AD), x-ray fluorescence (XRF), temperature programmed desorption (TPD), temperature programmed reduction (TPR), pulse chemisorption and surface area (BET and T-Plot).[31]

The PSD of the Ni/α-Al_2O_3 catalyst sample was measured using a Mastersizer 2000 from Malvern Instruments. The average particle size was assessed at 46.54 μm (d(0.5)). The apparent density of the catalyst was assessed to be 1929 kg/m^3, using a method established at CREC. Taking into consideration the PSD, AD, and Geldart's powder classification chart,[17] it was concluded that the Ni/α-alumina catalyst particles belong to the group A, a particle group considered to display good fluidization. These characteristics were further confirmed experimentally using a plexiglas model of the CREC riser simulator, specially manufactured for flow visualization.

XRF was used to estimate the metal loading of the catalyst. The XRF analysis was performed at the Dept. of Earth Sciences at The University of Western Ontario. The Ni loading of this catalyst was estimated at 3.3 wt %.

Temperature-programmed desorption (TPD) of ammonia was used to characterize the total acidity for both Ni/α-alumina catalyst and α-alumina. Ni/α-alumina catalyst displayed an acidity of 0.036 mmol NH_3/g, while α-alumina showed a higher 0.058 mmol NH_3/g value. This allows hypothesizing that nickel crystallites while covering the support acidic sites on the support surface, they reduce the total acidity of the α-alumina.

Temperature programmed reduction (TPR), and temperature programmed oxidation (TPO) sequential cycles show that, the Ni/α-alumina catalyst displays a single peak of reproducible magnitude centered at approximately 500°C. This result indicates a reducible phase primarily composed of NiO.[31]

The pulse chemisorption technique provides valuable information on the dispersion and on the crystal site of the supported metal. A pre-reduced sample of catalyst was used in order to perform the pulse chemisorption experiments. Quantitative results for the pulse chemisorption experiment are (a) metal dispersion was 3.4%, (b) metallic surface area were assessed at 0.6 m^2/g sample and 22.6 m^2/g metal, and (c) active particle diameter was estimated at 30 nm.

BET analysis on α-alumina (30.1 m^2/g sample), and the Ni/α-alumina catalyst (22.4 m^2/g sample) shows a moderate decrease in the total surface area of the catalyst after nickel is loaded on the calcined α-alumina support. The decrease of the surface area is assigned to the plugging of some of the support pores by nickel species.

Additional details regarding catalyst characterization can be found in Salaices.[31]

Glucose as surrogate model compound

Cellulose is the principal carbohydrate constituent of biomass. It is a polymer of glucose with a repeating unit of $C_6H_{10}O_5$ strung together by ß-glycosidic linkages. In a typical composition of biomass, cellulose ranges from 30 to 50 wt %.[13]

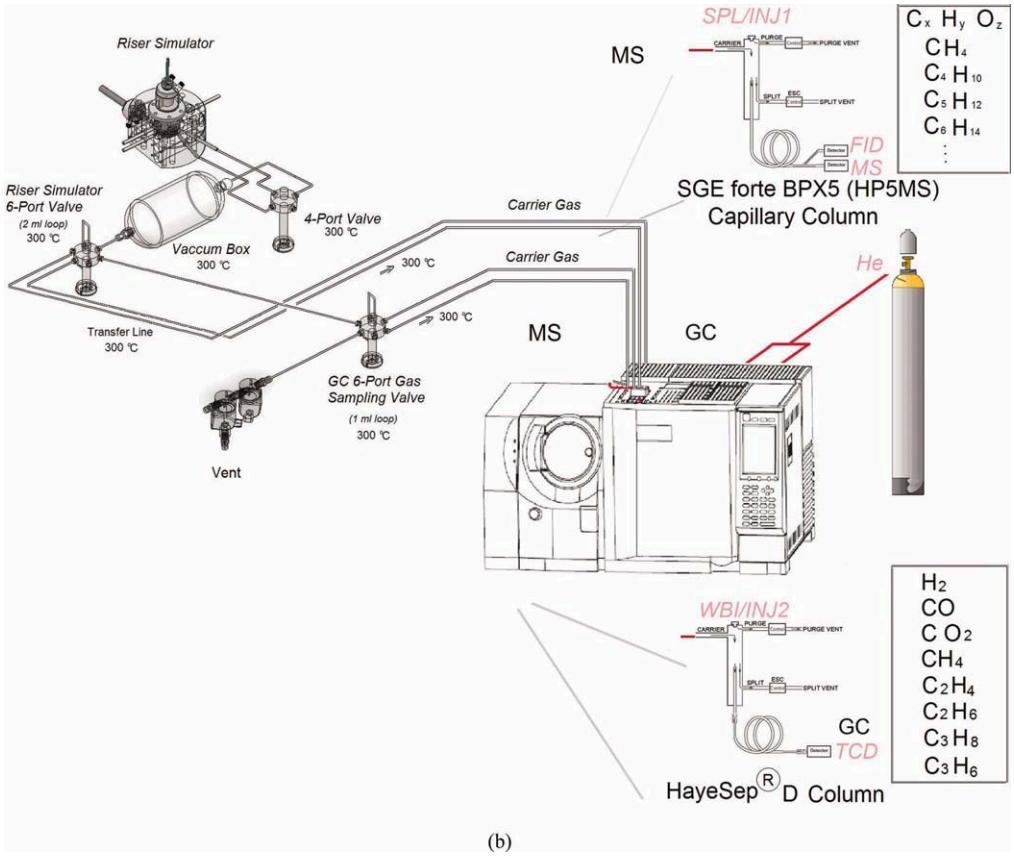

Figure 1. Continued

Glucose was used as model compounds of the cellulose contained in the biomass. Solution at steam/biomass ratios of 0.4, 0.6, 0.8, and 1.0 were prepared using high-purity D-(+)-glucose, minimum 99.5%, CAS 50-99-7 purchased from Sigma Aldrich, Inc., St. Louis.

Gasification runs in the CREC riser simulator

The gasification experimental runs were conducted in the CREC fluidized riser simulator (de Lasa[18]). Figure 1a reports the main characteristics of the CREC riser simulator: a bench-scale internal recycle batch reactor with a capacity of 53 cm^3 allowing the loading of 1 g of catalyst.

This reactor was designed in such way that an annular space is created between the outer portion of the basket and the inner part of the reactor shell. A metallic gasket seals the two chambers, and an impeller is located in the upper section. A packing gland assembly and a cooling jacket surround the shaft that supports the impeller. On rotation of the shaft, an inert gas is forced outward from the center of the impeller toward the walls. This creates a lower pressure in the center region of the impeller, thus, inducing a flow of gas upward through the catalyst chamber from the bottom of the reactor annular region where the pressure is slightly higher. The impeller of the CREC riser simulator provides a fluidized bed of catalyst particles as well as intense gas mixing inside the reactor.

As described in Figure 1b, a series of sampling valves complete the assembly of the CREC riser simulator and allow the withdrawal of reactants and products in short periods of time.

Figure 2a and 2b display typical pressure profiles in the CREC riser simulator as a result of the catalytic steam biomass gasification reaction when glucose was used as the biomass feedstock. Figure 2a display the pressure changes in the reactor (upper curves), and vacuum box (lower curves), simultaneously for a reaction time of 20 s, and for S/B ratios of 0.4, 0.6, 0.8, and 1.0. The vertical sections of the reactor pressure curves indicate the glucose-water injection into the reactor, and the release of the products into the vacuum box. As the S/B ratio increases for a set amount of glucose, Figure 2a shows increasingly higher pressure readings. The curved section of the graph (between the two vertical lines), represents the gasification period and displays an increase in pressure as the injected glucose compound cracks into various products. Figure 2b depicts the pressure changes in the reactor and vacuum box for the gasification of glucose when the S/B ratio remains constant at 0.8, and the reaction time varies from 5 to 30 s. The straight (vertical) and curved sections of this figure also denote the phenol injection/product release and the gasification reaction, respectively. For increasing reaction times, the curved sections of the graph become longer, but follow a consistent shape. The consistency of the shape of the curves, in both Figure 2a and b

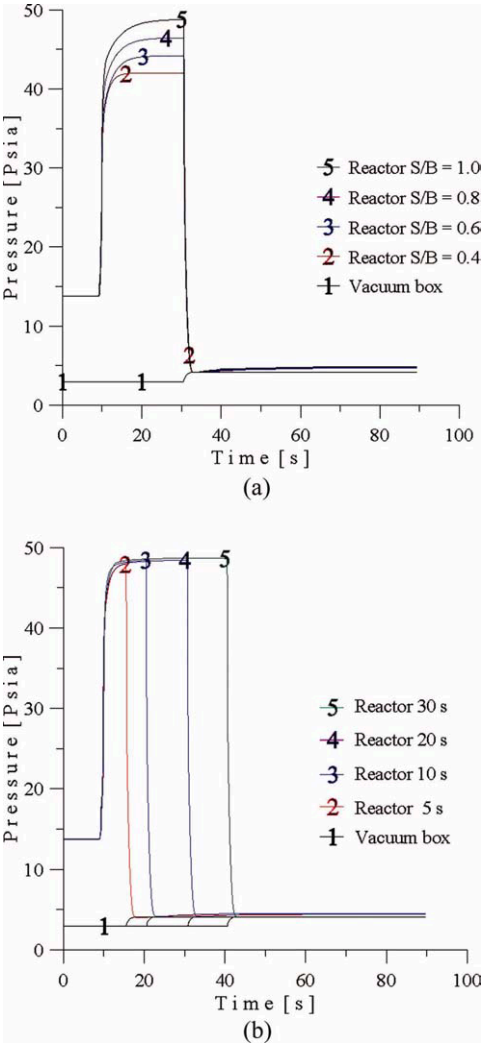

Figure 2. Change in pressure in CREC riser simulator for injection of 12.5 μL glucose at 650°C; (a) 20 s reaction times and steam/glucose ratios of 0.4, 0.6, 0.8, 1.0, and (b) steam/glucose ratio of 0.8, reaction times of 5, 10, 20 and 30 s.

[Color figure can be viewed in the online issue, which is available at wileyonlinelibrary.com.]

confirms that the CREC riser simulator produces precise results. The gaseous reaction products were analyzed in an Shimatzu 2010 GC/MS system.

The Shimatzu GC/TCD (thermal conductivity detector) with a packed column HayeSep® D 100/120 porous polymer, 30 ft × 1/8′ o.d. S.S. allows the separation and quantification of permanent gases (H_2, CO, CO_2, CH_4), and H_2O, C_2H_4, C_2H_6, C_2H_4O, and up to C_6 hydrocarbons. The Shimatzu mass spectrometer with a HP-5MS silica capillary column, 30 m × 0.25 m I.D. (5% phenyl-/95% methylpolysiloxane) permits the separation of the components present in the tars. The coke deposited on the catalysts was measured in a total organic carbon analyzer (TOC-V) with a solid sample module (SSM-5000) from Mandel.

Thermodynamic Analysis of Coke Formation

A mechanism generally accepted as the mode of carbon deposition on the catalyst/support structure involves the following reactions.[24–30]

As a result of these three reactions (reverse of Eqs. 6, 7, and 8) different amounts of coke may be formed with this depending on the S/B ratio and the operating temperature and pressure.

Methane pyrolysis is an endothermic reaction while water-gas shift and Boudouard reactions are exothermic (Table 1). To develop a thermodynamic analysis of the aforementioned coking reactions, their equilibrium constants were calculated according to the definition of the standard Gibbs energy change of reaction

$$\frac{d\Delta G^o}{RT} = -\ln K \tag{14}$$

$$\text{with } \Delta G^o = \Delta H_0^o - \frac{T}{T_o}(\Delta H_0^o - \Delta G_0^o) + R\int_{T_0}^{T}\frac{\Delta Cp^o}{R}dT - RT\int_{T_0}^{T}\frac{\Delta Cp^o}{R}\frac{dT}{T} \tag{15}$$

Therefore

$$\frac{d\ln K}{dT} = \frac{-\Delta H^o}{RT^2} \tag{16}$$

Equation 16 establishes the effect of temperature on the equilibrium constant, and, hence, on the equilibrium conversion.

Figure 3 reports the equilibrium constant for the carbon reaction considered in the equilibrium model at temperatures ranging from 600 to 700°C. In addition, three parameters can be defined using the experimental partial pressures at $P_o = 1$ atm

$$\alpha = \frac{(p_{H_2})^2}{p_{CH_4}}\frac{1}{P_o} \tag{17}$$

$$\beta = \frac{p_{CO_2}}{(p_{CO})^2}P_o \tag{18}$$

$$\gamma = \frac{p_{H_2O}}{p_{CO}p_{H_2}}P_o \tag{19}$$

It can be noticed that if $\alpha < K_1$, $\beta < K_2$ and $\gamma < K_3$ coke formation is thermodynamically allowed. This shows that in general, operating conditions for the gasification process are

Table 1. Coke Formation Reactions[11], the Reverse of Eqs (6), (7) and (8)

Name of reaction	Chemical equation	$\Delta G^o_{f(298)}$ [kJ/ mol]	$\Delta H^o_{f(298)}$ [kJ/ mol]
1 Heterogeneous water-gas shift	$H_2 + CO \longleftrightarrow C + H_2O$	−89.82	−130.41
2 Boudouard equilibrium	$2CO \longleftrightarrow C + CO_2$	−118.36	−172.62
3 Hydrogenating gasification reaction	$CH_4 \longleftrightarrow C + 2H_2$	50.27	74.90

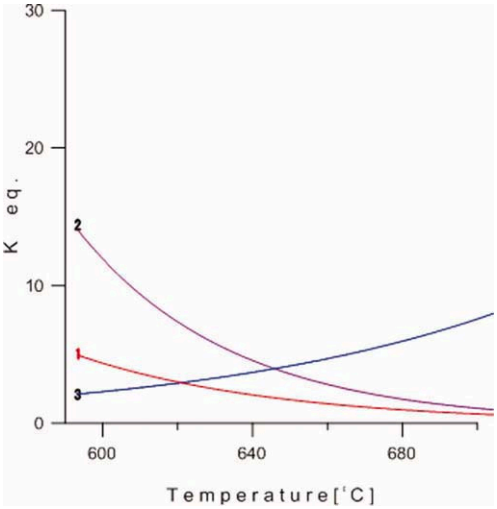

Figure 3. Equilibrium constant at different temperatures for (1) heterogeneous water-gas shift reaction, (2) Boudouard reaction, and (3) hydrogenating gasification reaction.

[Color figure can be viewed in the online issue, which is available at wileyonlinelibrary.com.]

sought to minimize the cases where α, β, and γ are smaller than their equilibrium constants.

Figure 4 through Figure 6 reports the trends of α, β and β vs. their respective equilibrium constants for a 30 s reaction time, steam/biomass (S/B) ratios of 0.4–1.0, 700°C, and P = 1 atm. The parameters α, β and γ were calculated from the partial pressures of H_2, CH_4, CO, CO_2, and H_2O for catalytic steam gasification of glucose in the CREC riser simulator.

One can notice that for the three reactions described in Figures 4, 5 and 6 the following occurs: (a) the $2CO \leftrightarrow C + CO_2$ and $CH_4 \leftrightarrow C + 2H_2$ are allowed with coke formation favored ($\alpha < K_1$ and $\beta < K_2$); and (b) the $CO + H_2 \leftrightarrow C + H_2O$ reaction is thermodynamically hindered with carbon conversion promoted ($\gamma > K_3$). As a result, a good approximation is to consider that on balance the net formation of carbon is negligible. This hypothesis is also consistent with

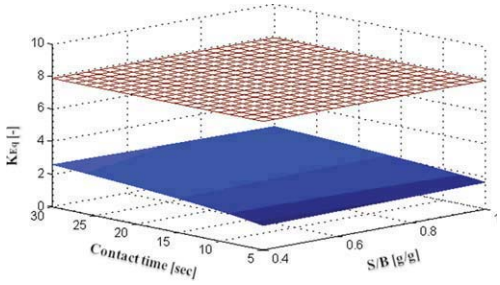

Figure 4. Expected trends for the equilibrium constant of the hydrogenating gasification reaction (reticulated surface), and the parameter α (plain surface) for various S/B ratio and reaction time at 700°C and 1 atm.

α surface was determined with more than 50 experimental data points. Note: $\alpha < K_1$ in all cases and as a result coke is allowed. [Color figure can be viewed in the online issue, which is available at wileyonlinelibrary.com.]

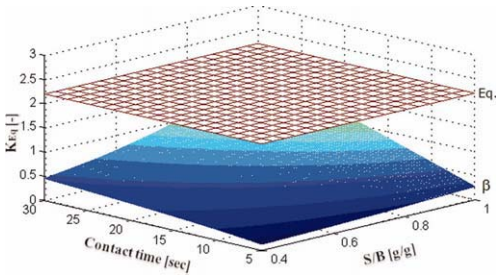

Figure 5. Expected trends for the equilibrium constant of the Boudouard equilibrium reaction (reticulated surface), and the parameter β (plain surface) with the S/B ratio and reaction time at 700°C and 1 atm.

β surface was determined with more than 50 experimental data points. Note: $\beta < K_2$ in all cases and as a result coke formation is allowed. [Color figure can be viewed in the online issue, which is available at wileyonlinelibrary.com.]

the very small amount of coke formed (<0.1 wt %) during the runs of this study.

On the aforementioned basis one can assume, as it will be done in the upcoming sections of this article, that negligible carbon species or carbon related reactions in the gasification kinetics need to be considered.

Overall Kinetic Model

The CREC riser simulator is a well-mixed batch reactor which operates under isothermal conditions.[10,20] Reaction rates for each component i can be expressed as follows

$$r_i = \frac{V}{W}\frac{d\left(\frac{p_i}{R\,T}\right)}{dt} \tag{20}$$

where V is the volume of the reactor in cm^3, W is the weight of the catalyst in grams, p_i is the partial pressure of specie i, R is the gas constant in cm^3 atm K^{-1} mol^{-1}, T is the reactor temperature in °K, and t is the time in seconds.

By combining Eqs. 10 and 20 a rate of reaction can be established for every chemical species as a function of partial pressures as follows

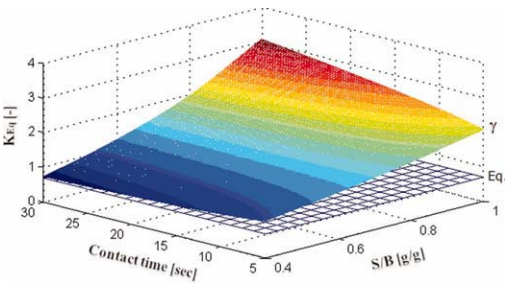

Figure 6. Expected trends for the equilibrium constant of the heterogeneous water-gas shift reaction (reticulated surface), and the parameter γ (plain surface), with the S/B ratio and reaction time at 700°C and 1 atm. β surface was determined with more than 50 experimental data points.

Note: $\gamma > K_3$ in all cases and as a result coke formation is not allowed. [Color figure can be viewed in the online issue, which is available at wileyonlinelibrary.com.]

$$\frac{d\left(\frac{p_i}{R\,\mathrm{T}}\right)}{dt} = \frac{\frac{W}{V} k_i^k K_j^A p_i}{\left(1 + \sum_{j=1}^{n} K_j^A p_j\right)^{m'}} \tag{21}$$

Let set $k_i' = \frac{W}{V} R\,T\,k_i^k K_j^A$, then Eq. 21 can be simplified to

$$\frac{dp_i}{dt} = \frac{k_i' p_i}{\left(1 + \sum_{j=1}^{n} K_j^A p_j\right)^{m'}} \tag{22}$$

with all k'_i rate constants in Eq. 22, representing kinetic constants which lump adsorption and intrinsic kinetic parameters.

However, if chemical species are involved in more than one reaction as it is described in Eq. 9 an equation of the form of Eq. 22 has to be considered for every relevant reaction step. This leads to a set of differential equations as reported in the next section.

Catalytic steam gasification postulated rate expression

The gathered gasification experimental data shows a negligible amount of carbon left on the catalyst and C_2^+ components in the product gas (i.e., <0.5 wt % for glucose at 700°C, SB 0.6, and 10 s of contact time). As a result, the reaction involving the gasification of C_2^+ hydrocarbons ($C_n H_{2m} + nH_2O \longrightarrow nCO + (n+m) H_2$), and the reaction including carbon $C + H_2O \longleftrightarrow H_2 + CO$, $C + CO_2 \longleftrightarrow 2CO$ and $C + 2H_2 \longleftrightarrow CH_4$ can be neglected.

Thus, once Eqs. 2, 6, 7 and 8 are discarded; the remaining reactions are the following (a) water-gas shift reaction or Eq. 3, (b) steam reforming of methane or Eq. 4, and (c) dry reforming of methane or Eq. 5. One can model the overall rate of formation/disappearance of every chemical species as an algebraic addition of individual relevant reactions

$$r_i = v_{WGS,i}\frac{r_{WGS,r}}{v_{WGS,r}} + v_{SR,i}\frac{r_{SR,r}}{v_{SR,r}} + v_{DRM,i}\frac{r_{DR,r}}{v_{DR,r}} \tag{23}$$

Moreover, one can consider the additional assumption that the CH_4 adsorption contribution to the kinetics is insignificant. This assumption was validated with adsorption experiments in the CREC riser simulator by Salaices.[31]

Thus, a set of differential equations to represent the catalytic steam gasification of biomass can be obtained including the WGS, SR and DRM reactions.

For instance, for hydrogen the overall rate of formation is given as follows:

$$\begin{aligned}\frac{dp_{H_2}}{dt} = &\frac{k'_{WGS}\,p_{CO}\,p_{H_2O}}{(1 + 2K^A_{CO_2}\,p_{CO_2})}\left(1 - \frac{p_{H_2}\,p_{CO2}}{K_{WGS}\,p_{CO}\,p_{H_2O}}\right)\\ &+ \frac{3\,k'_{SR} p_{CH_4} p_{H_2O}}{(1 + 4K^A_{CO_2} p_{CO_2})}\left(1 - \frac{p_{CO}\,p_{H_2}^3}{K_{SR}\,p_{CH_4}\,p_{H_2O}}\right)\\ &+ 2\,\frac{k'_{DRM}\,p_{CO_2}\,p_{CH_4}}{(1 + 4K^A_{CO_2}\,p_{CO_2})}\left(1 - \frac{p_{CO}^2\,p_{H_2}^2}{K_{DRM}\,p_{CO_2}\,p_{CH_4}}\right)\end{aligned} \tag{24}$$

where k_{WGS}, k_{SR} and k_{DRM} are the kinetic constants for the water-gas shift reaction (WGS), steam reforming reaction (SR), and dry reforming of methane reaction (DRM), respectively; K_{WGS}, K_{SR} and K_{DRM} are the thermodynamic equilibrium constants of the *WGS*, *SR* and *DRM* reactions at the reaction temperature; $K^A_{CO_2}$ is the adsorption constant for carbon dioxide, and p is the partial pressure of species i.

A similar equation can be written for each component in the product gas. The rate of formation and disappearance of carbon monoxide given by

$$\begin{aligned}\frac{dp_{CO}}{dt} = &-\frac{k'_{WGS}\,p_{CO}\,p_{H_2O}}{1 + 2K^A_{CO_2}\,p_{CO_2}}\left(1 - \frac{p_{H_2}\,p_{CO2}}{K_{WGS}\,p_{CO}\,p_{H_2O}}\right)\\ &+ \frac{k'_{SR}\,p_{CH_4}p_{H_2O}}{(1 + 4K^A_{CO_2}p_{CO_2})}\left(1 - \frac{p_{CO}\,p_{H_2}^3}{K_{SR}\,p_{CH_4}\,p_{H_2O}}\right)\\ &+ 2\,\frac{k'_{DRM}\,p_{CO_2}\,p_{CH_4}}{(1 + 4K^A_{CO_2}\,p_{CO_2})}\left(1 - \frac{p_{CO}^2\,p_{H_2}^2}{K_{DRM}\,p_{CO_2}\,p_{CH_4}}\right)\end{aligned} \tag{25}$$

For carbon dioxide, the reaction rate contribution of *WGS, SR* and *DRM* is written as

$$\begin{aligned}\frac{dp_{CO_2}}{dt} = &\frac{k'_{WGS}\,p_{CO}\,p_{H_2O}}{(1 + 2\,K^A_{CO_2}\,p_{CO_2})}\left(1 - \frac{p_{H_2}\,p_{CO2}}{K_{WGS}\,p_{CO}\,p_{H_2O}}\right)\\ &- \frac{k'_{DRM}\,p_{CO_2}\,p_{CH_4}}{(1 + 4K^A_{CO_2}\,p_{CO_2})}\left(1 - \frac{p_{CO}^2\,p_{H_2}^2}{K_{DRM}\,p_{CO_2}\,p_{CH_4}}\right)\end{aligned} \tag{26}$$

For water, the reaction rate contribution of *WGS* and *SR* is given by

$$\begin{aligned}\frac{dp_{H_2O}}{dt} = &-\frac{k'_{WGS}\,p_{CO}\,p_{H_2O}}{(1 + 2K^A_{CO_2}\,p_{CO_2})}\left(1 - \frac{p_{H_2}\,p_{CO_2}}{K_{WGS}\,p_{CO}\,p_{H_2O}}\right)\\ &- \frac{k'_{SR}\,p_{CH_4}p_{H_2O}}{(1 + 4K^A_{CO_2}p_{CO_2})}\left(1 - \frac{p_{CO}\,p_{H_2}^3}{K_{SR}\,p_{CH_4}\,p_{H_2O}}\right)\end{aligned} \tag{27}$$

Finally, the rate of formation and disappearance of methane is given by the reaction rate contribution of *SR* and *DRM* as follows

$$\begin{aligned}\frac{dp_{CH_4}}{dt} = &-\frac{k_{SR}p_{CH_4}p_{H_2O}}{(1 + 4K^A_{CO_2}p_{CO_2})}\left(1 - \frac{p_{CO}\,p_{H_2}^3}{K_{SR}\,p_{CH_4}\,p_{H_2O}}\right)\\ &- \frac{k'_{DRM}\,p_{CO_2}\,p_{CH_4}}{(1 + 4K^A_{CO_2}\,p_{CO_2})}\left(1 - \frac{p_{CO}^2\,p_{H_2}^2}{K_{DRM}\,p_{CO_2}\,p_{CH_4}}\right)\end{aligned} \tag{28}$$

In the CREC riser simulator chemical reactions can be studied in a wide range of time spans. Differential equations such as Eqs. 24–28 representing various chemical changes can be solved numerically for the complete span of reaction times (e.g., 5–30 s). Initial conditions at the product gas compositions at 5 s.

These postulated rate expressions inevitably lead to mathematical models that are nonlinear with respect to their parameters, particularly when the adsorption constants appear both in the numerator and in the denominator of the expression. The nonlinearity in the parameters can result in overparameterization given a high degree of parameter correlation. One shall notice that this parameter correlation is

Table 2. Adsorption Constant for Carbon Dioxide as a Function of Reaction Temperature

T [°C]	600	650	700
K^A_{CO2} [psia^{-1}]	9.12E-02	8.43E-02	7.80E-02

amplified given the mathematical form of the Langmuir-Hinshelwood equation where parameters to be fitted are both in the numerator and in the denominator of the rate equation.

One of the highlights of the mini-fluidized CREC riser simulator is given by the fact that the determination of adsorption and intrinsic kinetic parameters can be *decoupled*. As a result, one can obtain in the CREC riser simulator experimental data suitable for the analysis of either adsorption or reaction models with a limited number of parameters. This limited number of phenomenologically relevant parameters can be established with their respective statistical indicators: reduced parameter spans for the 95% confidence interval and low cross-correlation.

Kinetic parameter estimation

Adsorption Constants. The adsorption isotherms at various temperatures for methane and carbon dioxide were calculated independently using experimental data from the CREC riser simulator. This calculation related the equilibrium partial pressure of pure species with the adsorbed amounts of the same species. Table 2 reports the carbon dioxide adsorption constants at 600, 650 and 700°C when one gram of Ni/α-alumina was introduced into the CREC riser simulator's catalyst basket.

Once the adsorption parameter and its dependence with temperature was established, the intrinsic kinetic constants were estimated using the nonlinear least-squares regression routine *nlinfit.m*, available in the optimization toolbox of MATLAB, version 7.6.[21] This routine uses the Gauss-Newton algorithm with Levenberg-Marquardt modifications for global convergence. The integration of the differential system (24–28), required in the parameter estimation, was performed numerically using the *ode113* function; and the *nlparci* function was used to produce 95% confidence intervals for each estimated parameter.

Intrinsic Kinetic Constants. The reaction data, used to estimate the kinetic parameters corresponding to the surface reaction rates (k_i), was planned using Taguchi's design of experiments involving four factors (steam biomass ratio, reaction temperature, contact time, and total pressure), and three levels for each of the factors.

The conditions of the catalytic experiments when using glucose as a model compound for the cellulose contained in biomass, 0.4, 0.6, 0.8 and 1.0 steam/biomass ratios (g/g) wt %, 2 atm. of argon, catalyst/feedstock ratio of ~25, residences times: 5, 10, 20, and 30 s, and reaction temperatures 600, 650, and 700°C. All thermal and catalytic runs were repeated at least three times to secure reproducibility of results. An important observation from these runs was that the mass balance closures, which consider permanent gases (H_2, CO, CO_2, H_2O, and CH_4), ethylene, ethane, propylene, acetaldehyde, carbon deposited over the catalyst and tar, were in the ±5% range, with most of the balances in the ±2% range.

Table 3 reports the kinetic parameters for mixtures of glucose in water at S/B ratios of 0.4, 0.6, 0.8, and 1.0, as a function of the reaction temperature.

To obtain the intrinsic kinetic parameters (activation energies and pre-exponential factors), the kinetic parameters k_i and K_{CO2} (Eqs. 24–28) were allowed to vary with temperature using an Arrhenius relationship centered on an average temperature (650°C)

$$k_i = k^0{}_i \exp\left(-\frac{E_i}{R}\left(\frac{1}{T}-\frac{1}{T_{\text{avg}}}\right)\right) \tag{29}$$

$$K^A_{CO_2} = K^0{}_{CO_2} \exp\left(-\frac{\Delta H^{CO_2}_{\text{ads}}}{R}\left(\frac{1}{T}-\frac{1}{T_{\text{avg}}}\right)\right) \tag{30}$$

where k_i is the reaction rate constant of component i, K^0_i is the pre-exponential factor or reaction rate constant at 650°C, E_i is the activation energy, K^0_{CO2} is the carbon dioxide adsorption equilibrium constant at 650°C, $\Delta H^{CO2}_{\text{ads}}$ is the carbon dioxide heat of adsorption, R is the universal gas constant, and T_{avg} is the average temperature.

In terms of Eqs. 29 and 30, one should notice that the centered Arrhenius form reduces the correlation between the pre-exponential factor and the activation energy, thereby improving the statistical properties of the estimates for the pre-exponential factors.

Initial values for these intrinsic kinetic parameters to solve the new differential equation system were necessary. In this sense, the kinetic parameters at 650°C (Table 3) were used as pre-exponential guess values ($k^0{}_i$). Moreover, the initial activation energy (E_i) values were obtained from linear regression of the Arrhenius expressions (Eqs. 29 and 30) in a semilogarithmic plot. Finally, a total of six parameters ($k^0{}_{WGS}$, E_{WGS}, $k^0{}_{SR}$, E_{SR}, $k^0{}_{DRM}$, and E_{DRM}) were adjusted simultaneously by nonlinear multivariable regression of experimental data.

Table 4 summarizes the intrinsic kinetic parameters estimated with their 95% confidence interval, and the standard deviation of the residuals (σ).

By inspecting the results of the parameter estimation it can be noticed that the standard deviation (σ), calculated from the summation of the squares of the residuals, showing the quality of the fit. This result is particularly relevant given the number of parameters adjusted, and it is obtained as a result of the large number of data point's available (m).

Moreover, the intrinsic kinetic parameters corresponding to the rate-limiting surface reaction rates, k^0_i and E_i, are significant at the 95% confidence level, with this result showing that the reparameterization and temperature centering were successful in reducing the overall correlation between the parameters.

Table 3. Kinetic Parameters for Mixtures of Glucose in Water at Steam/Biomass (S/B) Ratios of 0.4, 0.6, 0.8, and 1.0, as a Function of the Reaction Temperature

T [°C]	600	650	700
k_{WGS}[a]	1.981E-06	3.07E-06	4.23E-06
k_{SR}[b]	4.39E-10	9.21E-10	1.45E-09
k_{DRM}[a]	1.13E-09	2.22E-09	3.24E-09

[a][mol gcat^{-1} s^{-1}], [b][mol gcat^{-1} s^{-1} psia^{-1}].

Table 4. Intrinsic Kinetic Parameters of the Proposed "Additive" Kinetic Model With Their 95% Confidence for WGS, DRM and SRM Reactions

Glucose		
Parameter	Value	Span for 95% confidence
k^0_{WGS} [a]	3.07×10^{-6}	$\pm 2.14 \times 10^{-7}$
E_{WGS} [b]	53.1	±1.28
k^0_{SR} [c]	9.21×10^{-10}	$\pm 2.38 \times 10^{-10}$
E_{SR} [b]	93.0	±56.5
k^0_{DRM} [c]	2.22×10^{-09}	$\pm 1.69 \times 10^{-10}$
E_{DRM} [b]	75.8	±14.8
K^o_{CO2} [d]	8.43×10^{-2}	$\pm 1.91 \times 10^{-3}$
ΔH^A_{CO2} [b]	−11.01	±6.1
σ [e]	1.48×10^{-3}	
m	240	

[a][mol gcat^{-1} s^{-1} psia^{-1}]; [b][kJ/mol]; [c][mol gcat^{-1} s^{-1}]; [d][psia^{-1}]; [e]$\sigma = \sqrt{\sum (X_{\text{experimental}} - X_{\text{estimated}})^2/(m-p)}$, where m is the number of data points and p is the number of model parameters.

The activation energies calculated display signs consistent with the expected dependence of these constants with temperature. Positive E_{SR} and E_{DRM} signs show a methane conversion intrinsic constant favored by higher temperatures. A negative sign shows a CO_2 adsorption process negatively affected by temperature increases.

Regarding the energies of activation (E_i), it is important to review the magnitude of the activation energies obtained in the context of this study and compare them with energies of activation for the same water-gas shift, steam methane reforming and dry methane reforming reported in the literature. This comparison is reported in Table 5.

Concerning water-gas-shift reaction (WGS) activation energies, the values reported are in the 39.3 to 55.5 kJ/mol ranges when using a WGS rate formulation including chemical equilibrium and stepwise model type rate equation. Taking into consideration the span for 95% confidence reported, the parameter spans include the 53.1 kJ/mol activation energies calculated using glucose. As a result, the calculated parameters are well in line with the data available in the literature.

Regarding steam reforming of methane (SRM), the activation energies for the dissociation of CH_4 on Ni range from 70 to 141 kJ/mol. As a result the activation energy of 93.0 kJ/mol determined in this study for glucose is in agreement with literature data.

For the dry reforming of methane (DRM) Michael et al.[21] report activation energies in the 93.3 to 123.2 kJ/mol range for similar nickel-based catalysts. These values include the 75.8 kJ/mol activation energies calculated for DRM reaction using glucose model compound. Thus, the calculated parameters for DRM can be considered reasonably in line with the data from the literature.

In conclusion, it can be stated that the proposed kinetic model provides sound energies of activations in the case of glucose for the WGS, DRM and SRM dominant reactions.

Gasification kinetic modeling results

The experimental and model-predicted values for glucose gasification, using the intrinsic kinetic parameters reported in Table 4 are shown in Figures 7 through Figure 11.

One important issue to address while applying this model is the initial conditions for the kinetic calculation. Thanks to the principle of operation of the CREC riser simulator, where reaction time can be changed in a wide range of values, from 5 s to 30 s, and considering the gas composition at 5 s or the shortest reaction time, various stoichiometric coefficients in Eq 1 was set at reaction time approaching zero. With this information and the intrinsic kinetic and adsorption parameters established, the various differential equations (Eqs. 24–28) were solved numerically.

Numerical solution of these equations shows that the proposed kinetic model gives accurate predictions of the partial pressure of product permanent gases (H_2, CO, CO_2, H_2O and CH_4). Figures 7 through 11 report a reasonably random distribution of the product permanent gases with respect to the 45° perfect agreement case, with this result indicating that all individual products are predicted satisfactorily.

On this basis, it can be concluded that the set of adsorption and kinetic parameters established is adequate for predicting hydrogen, carbon monoxide, carbon dioxide, methane and water concentrations.

It can also be concluded that given the sound reaction engineering basis of the proposed kinetic model, it could likely be successfully used for biomass conversion predictions in circulating fluidized-bed gasifiers.

Table 5. Activation Energy Review with the Reported in the Literature [kJ/mol]for Water-Gas Shift Reaction, Steam Reforming of Methane and Dry Reforming of Methane

Water Gas-Shift reaction		
This study Glucose [L-H]	Literature WGS_{eq} form – [Stepwise]	Reference
53.1 [±1.28]	39.3 [±13.4] – 55.5 [±12.2]	Mark et al.[22]
	Steam Reforming of Methane reaction	
This study Glucose [L-H]	Literature [L-H] – [ER II]	Reference
93.0 [±56.5]	70 – 141 [±51.0]	Nikolla et al.[23]; Jarosch et al.[24]
	Dry Reforming of Methane reaction	
This study Glucose [L-H]	Literature [L-H] - Stepwise	Reference
75.8 [±14.8]	93.2 [±27.9] – 123.2 [±4.7]	Mark et al.[22]

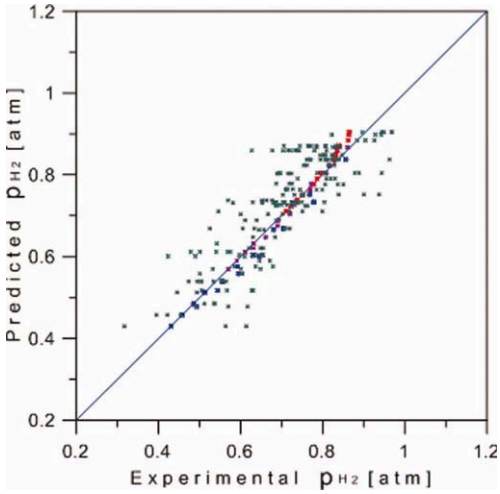

Figure 7. Predicted and experimental hydrogen yields from catalytic steam gasification of glucose over Ni/α-alumina at various temperatures, residence times, and steam biomass ratios.

[Color figure can be viewed in the online issue, which is available at wileyonlinelibrary.com.]

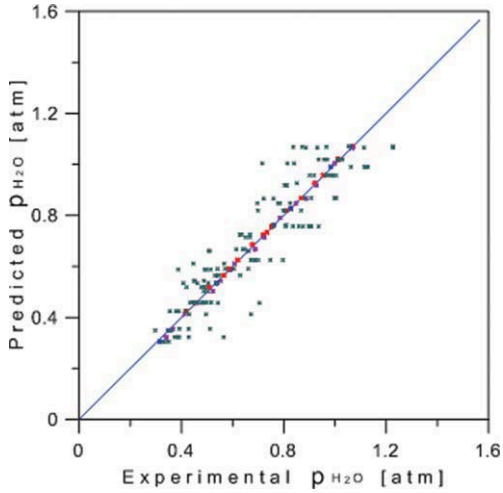

Figure 9. Predicted and experimental water yields from catalytic steam gasification of glucose over Ni/α-alumina at various temperatures, residence times, and steam biomass ratios.

[Color figure can be viewed in the online issue, which is available at wileyonlinelibrary.com.]

Conclusions

(a) It is shown that a three reaction additive kinetic model is adequate to represent the steam gasification of biomass over Ni/α-alumina. The model proposed successfully accounts for various product gas species (H_2, CO, CO_2, H_2O and CH_4).

(b) It is proven that the experimental-modeling procedure, where intrinsic kinetic parameters and adsorption constants are *decoupled* in their evaluation as accomplished in the CREC riser simulator eliminates overparameterization.

(c) It is demonstrated that the centered Arrhenius exponential term reduces correlation between the pre-exponential factor and the activation energy, thereby improving the statistical properties of the estimates for both activation energy and pre-exponential factor.

(d) It is proven that the resulting energies of activation in the case of glucose gasification are in agreement in their magnitudes with those reported in the literature using single component reactions. This shows the likelihood that the proposed model includes phenomenologically based parameters that can be linked to intrinsic reaction kinetics.

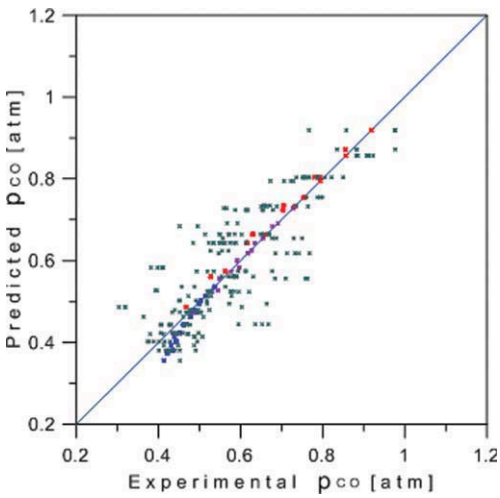

Figure 8. Predicted and experimental carbon monoxide yields from catalytic steam gasification of glucose over Ni/α-alumina at various temperatures, residence times, and steam biomass ratios.

[Color figure can be viewed in the online issue, which is available at wileyonlinelibrary.com.]

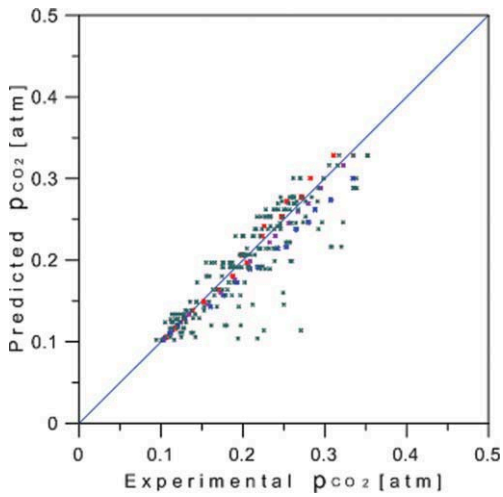

Figure 10. Predicted and experimental carbon dioxide yields from catalytic steam gasification of glucose over Ni/α-alumina at various temperatures, residence times, and steam biomass ratios.

[Color figure can be viewed in the online issue, which is available at wileyonlinelibrary.com.]

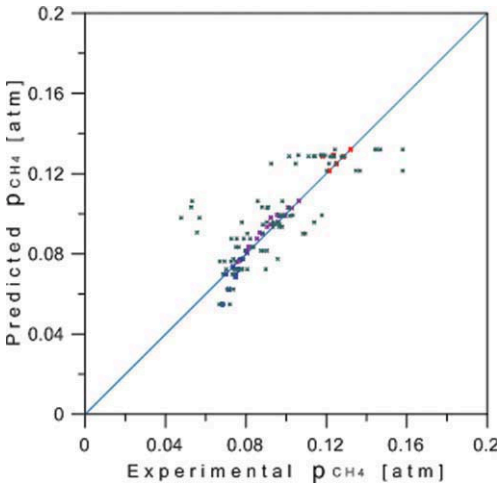

Figure 11. Predicted and experimental methane yields from catalytic steam gasification of glucose over Ni/α-alumina at various temperatures, residence times, and steam biomass ratios.

[Color figure can be viewed in the online issue, which is available at wileyonlinelibrary.com.]

Acknowledgments

We would like express our thanks to the Mexican Government (FGS-CONACyT) and the U.W.O. Faculty of Graduates Studies for the scholarships awarded to Enrique Salaices to pursue his Ph.D. studies at the University of Western Ontario. We would also like to express our appreciation to the Natural Sciences and Engineering Research Council of Canada NSERC and to the ABIN-Canada program for the financial support provided to this research. Professor B. Serrano would like to thank the Mexican federal program P/PIFI-2009-32MSU0017H-07 for their generous support of this research.

Notation

AD = apparent density
BET = Brunauer, Emmett and Teller method
CREC = chemical reaction engineering center
DRM = dry reforming of methane reaction
E_i = activation energy in *kJ*/mol
GC = gas chromatography
j = subscript to denote each component
k'_i = kinetic constant lumping adsorption and intrinsic kinetic parameters
K_i^k = kinetic constant for component "i" in mol/g_{cat} min
K_i^0 = pre-exponential factor
k_{DRM} = Intrinsic kinetic constant for the dry reforming of methane
k'_{DRM} = kinetic constant for the dry reforming of methane, $k_{DRM}K^A_{CH_4}K^A_{CO_2}$
k_{SRM} = intrinsic kinetic constant for the steam reforming of methane
k'_{SRM} = kinetic constant for steam reforming of methane, $k_{SRM}K^A_{CH_4}K^A_{H_2O}$
k_{WGS} = intrinsic kinetic constant for the dry reforming of methane
k'_{WGS} = kinetic constant for water gas shift reaction, $k_{WGS}K^A_{CO}K^A_{H_2O}$
K_i^A = adsorption constant for component "i" in 1/atm
K_{WGS} = equilibrium constant for the water gas shift reaction
K_{SR} = equilibrium constant for the steam reforming of methane
K_{DRM} = equilibrium constant for the dry reforming of methane
m = number of data points
m' = number of sites involved in the catalytic reaction
MS = mass spectrometer
n = number of chemical species
Ni = nickel
NiO = nickel oxide
Ni/α-Al_2O_3 = nickel supported on alpha-alumina
NR = Newton-Raphson
p_i = partial pressure of component i in atm
PSD = particle-size distribution
r_i = rate of reaction of component i in mol/g_{cat} min
$r_{WGS,H2}$ = water-gas shift reaction rate, Eqs. 3 and 11, based on H_2 formed
$r_{SR,CO}$ = steam reforming of methane reaction rate (Eqs 4 and 12) based on CO formed
$r_{DRM,CH4}$ = dry reforming of methane reaction rate (Eqs. 5 and 13) based on CH_4 consumed
R = gas constant in atm cm^3 mol^{-1} K^{-1}
S/B = steam biomass ratio in g/g
SR = steam reforming of methane reaction
σ = standard deviation
SSM = solid sample module
t = time in seconds
T = temperature in °K
T_{ave} = average temperature in °K
TOC = total organic carbon analyzer
TPD = temperature programmed desorption
TPR = temperature programmed reduction
TCD = thermal conductivity detector
V = reactor volume in cm^3
W = catalyst weight in grams
WGS = water-gas shift reaction
XRD = x-ray diffraction

Greek letters

$$\alpha = \frac{p_{H_2}^2}{p_{CH_4}}\frac{1}{P_o}$$

$$\beta = \frac{p_{CO_2}}{p_{CO}^2}P_o$$

$$\gamma = \frac{p_{H_2O}}{P_{CO}p_{H_2}}P_o$$

ΔH_{ads}^{CO2} = carbon dioxide heat of adsorption
$v_{WGS,i}$ = stoichiometric coefficient for the chemical species i involved in water-gas shift reaction
$v_{WGS,r}$ = stoichiometric coefficient for the reference chemical species in water-gas shift reaction (positive 1, based on H_2)
$v_{SR,i}$ = stoichiometric coefficient for the chemical species i involved in steam reforming
$v_{SR,r}$ = stoichiometric coefficient for the reference chemical species in steam reforming (positive 1, based on CO formed)
$v_{DR,i}$ = stoichiometric coefficient for the chemical species "i" involved in dry reforming
$v_{DR,r}$ = stoichiometric coefficient for the reference chemical species in dry reforming (negative 1, based on CH_4 consumed)

Literature Cited

1. Franco C, Pinto F, Gulyurtlu I, Cabrita I. The study of reactions influencing the biomass steam gasification process. *Fuel*. 2003;82(7):835–842.
2. Munir S, Daood S, Nimmo W, Cunliffe A, Gibbs B. Thermal analysis and devolatilization kinetics of cotton stalk, sugar cane bagasse and shea meal under nitrogen and air atmospheres. *Bioresour Technol*. 2009;100(3):1413–1418.
3. Salaices E, Serrano B, de Lasa H. Biomass catalytic steam gasification thermodynamic analysis and reactor experiments in a CREC riser simulator. *Ind Eng Chem Res*. 2010;49(15):6834–6844.
4. Fiaschi D, Michelini M. A two-phase one-dimensional biomass gasification kinetics model. *Biomass Bioenergy*. 2001;21(2):121–132.
5. Radmanesh R, Chaouki J, Guy C. Biomass gasification in a bubbling fluidized bed reactor: experiments and modeling. *AIChE J*. 2006;52(12):4258–4272.
6. Corella J, Sanz A. Modeling circulating fluidized bed biomass gasifiers: a pseudo-rigorous model for stationary state. *Fuel Process Technol*. 2005;86(9):1021–1053.
7. Orfao J, Antunes JM, Figueiredo JL. Pyrolysis kinetics of lignocellulosic materials - three independent reactions model. *Fuel*. 1999;78(3):349–358.

8. Aznar MP, Caballero MA, Gil J, Martin JA, Corella J. Commercial steam reforming catalysts to improve biomass gasification with steam-oxygen mixtures: catalytic tar removal. *Ind Eng Chem Res.* 1998;37(7):2668–2680.
9. Perez PP, Aznar PM, Caballero MA, Gil J, Martin JA, Corella J. Hot gas cleaning and upgrading with a calcined dolomite located downstream a biomass fluidized bed gasifier operating with steam - oxygen mixtures. *Energy Fuels.* 1997;11(6):1194–1203.
10. Ginsburg J, de Lasa H. Catalytic gasification of biomass in crec fluidized riser simulator. *Int J Chem Reactor Eng.* 2005;3:A38.
11. Schuster G, Loffler G, Weigl K, Hofbauer H. Biomass steam gasification - an extensive parametric modeling study. *Bioresour Technol.* 2001;77(1):71–79.
12. Li XT, Grace JR, Lim CJ, Watkinson AP, Chen HP, Kim JR. Biomass gasification in a circulating fluidized bed. *Biomass Bioenergy.* 2004;26(2):171–193.
13. McKendry P. Energy production from biomass (part 1): Overview of biomass. *Bioresource Technol.* 2002;83:37–46.
14. Rapagna S, Jand N, Kiennemann A, Foscolo PU. Steam-gasification of biomass in a fluidized-bed of olivine particles. *Biomass Bioenergy.* 2000;19(3):187–197.
15. Ruggiero M, Manfrida G. An equilibrium model for biomass gasification processes. *Renewable Energy.* 1999;16(1–4):1106–1109.
16. Kilpinen P, Hupa M, Leep alahti J. Nitrogen Chemistry at Gasification. A Thermodynamic Analysis. Combustion Chemistry Research Group Report, Abo Academi University, Finland; 1991:91–114,
17. Geldart D, Types of gas fluidization. *Powder Technol.* 1973;7(5): 285–292.
18. de Lasa H. Riser simulator for catalytic cracking studies. US Patent 5,102,678, 1992.
19. Ollis DF, Pelizzeti E, Serpone N. *Heterogeneous Photocatalysis in the Environment: Application to Water Purification. Photocatalysis Fundamentals and Applications.* Wiley Interscience. New York, NY: John Wiley & Sons; 1989:603–637.
20. Pekediz A, Kraemer DW, Chabot J, de Lasa HI. *Mixing Patterns in a Novel Riser Simulator*. In: de Lasa HI, Dogu G, Ravella A, eds. *Chemical Reactor Technology for Environmentally Safe Reactors and Products.* Applied Sciences Series. Kluwer Academic Press. 1992;225:133–46.
21. MATLAB version 7.6.0.324 (R2008a). The Matworks, Inc; 2008.
22. Mark FM, Mark F, Maier W. Reaction kinetics of the $C0_2$ reforming of methane. *Chem Eng Technol.* 1997;20(6):361–370.
23. Nikolla E, Schwank J, Linic S. Comparative study of the kinetics of methane steam reforming on supported Ni and Sn/Ni alloy catalysts: The impact of the formation of Ni alloy on chemistry. *J Catal.* 2009;263(2):220–227.
24. Jarosch K, El Solh T, de Lasa H. Modeling the catalytic steam reforming of methane: discrimination between kinetic expressions using sequentially designed experiments. *Chem Eng Sci.* 2002; 57(16):3439–3451.
25. Rostrup-Nielsen J, Hansen JB. CO_2-reforming of methane over transition metals. *J Catal.* 1993;144(1):38–49.
26. Wang S, Lu GQ. Carbon dioxide reforming of methane to produce synthesis gas over metal-supported catalysts: state of the art. *Energy Fuels.* 1996;10(4):896–894.
27. Bradford MCJ, Vannice MA. Catalytic reforming of methane with carbon dioxide over nickel catalysts I. Catalyst characterization and activity. *Appl Catal A.* 1996;142(1):73–96.
28. Pinaeva L, Schuurman Y, Mirodatos C. Carbon Routes in Carbon Dioxide Reforming of Methane. 221st National Meeting of the American Chemical Society, April 1–5, 2001; San Diego, CA. Environmental Challenges and Greenhouse Gas Control for Fossil Fuel Utilization in the 21st Century. 2002: 313–327.
29. Olsbye U, Moen O, Slagtern A, Dahl JM. An investigation of the coking properties of fixed and fluid bed reactors during methane-to-synthesis gas reactions. *Appl Catal A.* 2002:228(1–2);289–303.
30. Liu BS; Au CT. Carbon deposition and catalyst stability over La_2NiO_4/gamma-Al_2O_3 during CO_2 reforming of methane to syngas. *Appl Catal A.* 2003;244(1):181–195.
31. Salaices E. Catalytic Steam Gasification of Biomass Surrogates: a Thermodynamic and Kinetic Approach. [Ph.D Dissertation]. University of Western Ontario, Canada; 2010.
32. Campbell CT, Daube KA. A surface science investigation of the water-gas shift reaction of copper. *Surface Sci.* 1987;541(1–3):21–30.
33. El Solh T, Jarosch K, de Lasa H. Fluidizable Catalyst for Methane Steam Reforming. *Appl Catal A.* 2001;20(1–2), 351–324.
34. Xu G, Froment G. Methane steam reforming. methanation and water-gas shift: intrinsic kinetics. *AIChE J.* 1989:35(1);88–96.
35. Munster P, Grabke H. Kinetics of steam reforming of methane with iron, nickel and iron-nickel alloys as catalysts. *J Catal.* 1981;72(2): 279–287.
36. El Solh T, Jarosch K, de Lasa H. Catalytic dry reforming of methane in a crec riser simulator: kinetic modeling and model discrimination. *Ind Eng Chem Res.* 2003;42:2507–2515.

Manuscript received Feb. 8, 2011, and revision received May 11, 2011.